Available online at www.sciencedirect.com
ScienceDirect
Biochimica et Biophysica Acta 1767 (2007) 565–574
Biochimica et Biophysica Acta
BBA
www.elsevier.com/locate/bbabio

Photosynthetic dioxygen formation studied by time-resolved delayed fluorescence measurements — Method, rationale, and results on the activation energy of dioxygen formation

Joachim Buchta, Markus Grabolle, Holger Dau *

Freie Univ. Berlin, FB Physik, Arnimallee 14, D-14195 Berlin, Germany

Received 14 November 2006; received in revised form 30 March 2007; accepted 16 April 2007
Available online 24 April 2007

Abstract

The analysis of the time-resolved delayed fluorescence (DF) measurements represents an important tool to study quantitatively light-induced electron transfer as well as associated processes, e.g. proton movements, at the donor side of photosystem II (PSII). This method can provide, inter alia, insights in the functionally important inner-protein proton movements, which are hardly detectable by conventional spectroscopic approaches. The underlying rationale and experimental details of the method are described. The delayed emission of chlorophyll fluorescence of highly active PSII membrane particles was measured in the time domain from 10 μs to 60 ms after each flash of a train of nanosecond laser pulses. Focusing on the oxygen-formation step induced by the third flash, we find that the recently reported formation of an S4-intermediate prior to the onset of O–O bond formation [M. Haumann, P. Liebisch, C. Müller, M. Barra, M. Grabolle, H. Dau, Science 310, 1019–1021, 2006] is a multiphasic process, as anticipated for proton movements from the manganese complex of PSII to the aqueous bulk phase. The S4-formation involves three or more likely sequential steps; a tri-exponential fit yields time constants of 14, 65, and 200 μs (at 20 °C, pH 6.4). We determine that S4-formation is characterized by a sizable difference in Gibbs free energy of more than 90 meV (20 °C, pH 6.4). In the second part of the study, the temperature dependence (−2.7 to 27.5 °C) of the rate constant of dioxygen formation (600/s at 20 °C) was investigated by analysis of DF transients. If the activation energy is assumed to be temperature-independent, a value of 230 meV is determined. There are weak indications for a biphasicity in the Arrhenius plot, but clear-cut evidence for a temperature-dependent switch between two activation energies, which would point to the existence of two distinct rate-limiting steps, is not obtained.

Keywords: Chlorophyll fluorescence; Delayed fluorescence; Oxygen evolution; Oxygenic photosynthesis; Photosystem II; Water oxidation

1. Introduction

Photosystem II (PSII) is a complex of numerous cofactors (>70) and more than 20 protein subunits. It is embedded in the thylakoid membrane of plants and cyanobacteria. Driven by four light quanta, in PSII two water molecules are oxidized and two plastoquinones are doubly reduced. The catalytic site of water oxidation involves a Mn_4Ca complex ligated by distinct amino acids of the PSII complex. Identification of ligating amino acids became possible by the recent progress in crystallographic characterization of the evolutionary largely conserved core complex of PSII [1–4]. This remarkable progress crowned the long-standing quest for a structural PSII model of Horst Witt (and his Berlin coworkers) and Jim Barber

Abbreviations: AD, analog-to-digital (conversion); Chl, chlorophyll; DCBQ, 2,6-Dichloro-1,4-benzoquinone; EPPS, 4-(2-Hydroxyethyl)piperazine-1-propanesulfonic acid; DF, delayed fluorescence; ET, electron transfer; F_D, delayed fluorescence signal; F_P, prompt fluorescence signal; F_M, maximum level of prompt fluorescence; F_0, minimum level of prompt fluorescence; fwhm, full-width at half maximum; ΔG, difference in Gibbs' free-energy; MES, 2-Morpholinoethanesulfonic acid; MOPS, 3-Morpholinopropanesulfonic acid; P680, primary chlorophyll donor in PSII; Phe, specific pheophytin of PSII; PM, photomultiplier; PSII, Photosystem II; Q_A, primary quinone acceptor of PSII; Q_B, secondary quinone acceptor of PSII; Z or Y_Z or Tyr_Z, Tyr-160/161 of the D1 protein of PSII

* Corresponding author. Tel.: +49 30 838 53581; fax: +49 30 838 56299.
E-mail address: holger.dau@physik.fu-berlin.de (H. Dau).

0005-2728/$ - see front matter © 2007 Elsevier B.V. All rights reserved.
doi:10.1016/j.bbabio.2007.04.003

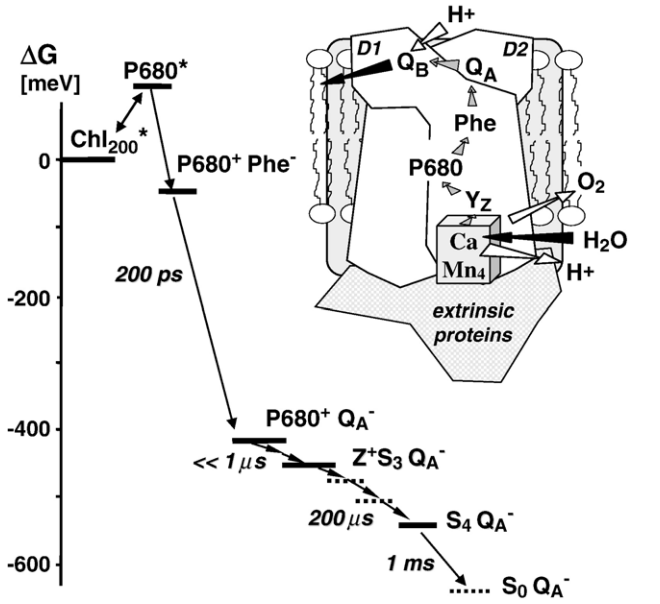

Fig. 1. Energy-level diagram of radical-pair states in photosystem II. The Gibbs free-energy is given for the states that are formed after the third photon absorption events, which initiates dioxygen-formation in the $S_3 \rightarrow S_0$ transition. The zero-level of the free-energy scale corresponds to the excited state of the chlorophyll antenna, which is lower than the P680* level due to the antenna-entropy contribution [10,11]. The free-energy level of the state labeled as $S_0Q_A^-$ is unknown, it may depend on the oxygen partial pressure [12,13]. Approximate values of characteristic halftimes are indicated. For determination of the free-energy levels, see [14] and references therein; the ΔG of the $S_3 \rightarrow S_4$ transition is determined in the present investigation. The inset illustrates the location of the various redox-factors in the PSII complex.

(and his coworkers in London). In the light of these breakthroughs in structure elucidation, which have delivered a detailed but static picture of PSII, kinetic studies focusing the still insufficiently understood mechanism of photosynthetic water have gained importance. Recently we have described the method [5–8] and reported results obtained by time-resolved X-ray absorption measurements with microsecond resolution [9]. In the present study, an approach for using delayed-fluorescence time courses is described for obtaining complementary insights in both, the kinetics (rate constants) and energetics (free-energy differences) of the processes at the donor side of PSII.

After absorption of a photon by one of the antenna pigments, the excited state is rapidly transferred to the PSII reaction center where the primary electron transfer results in reduction of a specific pheophytin and oxidation of P680, the primary chlorophyll donor (see Fig. 1). Within less than a nanosecond Q_A, a firmly bound quinone molecule, is reduced. Formation of the (Q_A^-, $P680^+$) radical pair is followed by electron transfer from the Tyr-160/161 of the D1 protein of PSII, which in the following is denoted as Y_Z, to $P680^+$. The (Q_A^-, $Y_Z^{\bullet+}$) radical state is formed within less than 1 μs. Clearly later, electrons are transferred from the Mn_4Ca complex to the Y_Z radical, the corresponding time constants are given in Fig. 2. The processes at the electron-donor side of PSII that follow the $Y_Z \rightarrow P680$ electron transfer are discussed in the framework of the S-state model introduced in a seminal study by Bessel Kok and his coworkers [15].

The classical S-state cycle involves five intermediate states (Fig. 2). The dark-stable S_1 state and the semi-stable states S_2, S_3 and S_0 have been studied intensely. By time-resolved X-ray absorption measurements, recently the formation of a reaction intermediate formed prior to the onset of O–O bond formation has been resolved [9]. In Fig. 2, this intermediate is denoted as S_4-state and the classical S-state cycle is extended by an S_4' state. We emphasize that the $S_3 \rightarrow S_4$ transition of Fig. 2 differs form the other $S_i \rightarrow S_{i+1}$ transition (for a discussion see Supporting Online Material of [9] and [18]). The $S_3 \rightarrow S_4$ transition most likely involves a proton removal from the Mn_4Ca, but not a one-electron oxidation of the Mn_4Ca complex. In contrast, the other $S_i \rightarrow S_{i+1}$ transition either involve both electron and proton removal from the Mn complex (meaning oxidation as well as deprotonation) or solely a oxidation step (in the $S_1 \rightarrow S_2$ transition) (see [17] in this issue). Recently we proposed a reaction cycle of photosynthetic dioxygen formation involving strictly alternate removal of four electron and four protons from the Mn complex [16,17]. This basic model explains the intricate proton release pattern and kinetic properties of the individual S-state transitions in a surprisingly simple way. It also may resolve the nomenclature problem by obliterating the need for a potentially ambiguous assignment of the S_4-state of Bessel Kok. (In the present work the nomenclature proposed in [9] is used where the new kinetically resolvable reaction intermediate has been denoted as S_4-state.)

In [9,18], the $S_3 \rightarrow S_4$ transition has been assigned to a deprotonation of the Mn complex or its immediate ligand environment that is electrostatically driven by the positive charge at or close to the $Y_Z^{\bullet}$ radical. Experimental evidence for the relation to a multi-step proton release process came (*inter alia*) from the analysis of time-resolved delayed fluorescence (DF) measurements (see Supporting Online Material of [9]), a method which had been used in the past for studies on PSII

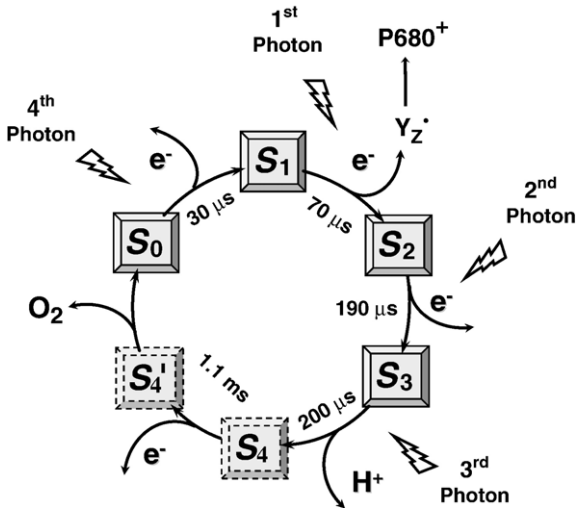

Fig. 2. Extension of the classical S-state cycle of photosynthetic oxygen evolution (modified from [9]). Each flash causes oxidation of Y_Z, prior to the indicated S-state transition. We note that the S_4-state is not formed by electron transfer to the Y_Z radical, but supposedly by a deprotonation triggered by the positive charge at the Y_Z radical. Proton release not representing a distinct, rate-limiting step has been omitted in the shown scheme. For a complete reaction cycle including also the four proton release steps, see [16,17].

water oxidation [19–25]. In the first part of the present work we show how DF measurement and analysis facilitates determination of the mean rate of S_4-formation, of the associated drop in free energy, and of the rate constant of dioxygen formation (in the $S_4 \rightarrow S_4' \rightarrow S_0$ transition). The focus lies on the description of the methodical approach.

In the second part of this study, the temperature dependence of the rate constant of dioxygen formation (k_{ox}) is investigated – in search of a breakpoint behavior with distinctly different activation energies below and above the breakpoint temperature. An activation energy of 208 meV above 6 °C and of 477 meV below 6 °C has been reported in [26] for PSII membrane fragments, but was not observed in [27]. We note that a breakpoint behavior in the temperature dependence of k_{ox} would be of high interest. It might indicate a change of the rate-limiting step in a sequence of two reactions in dioxygen formation.

2. Materials and methods

2.1. PSII membrane particles and buffer media

Highly active PSII membrane particles were prepared from spinach as described in [28] and stored at −80 °C at a Chl concentration of 1.5–2.5 mg Chl/mL in a buffer containing 1 M glycine betaine, 15 mM NaCl, 5 mM $MgCl_2$, 5 mM $CaCl_2$, and 25 mM MES, pH 6.2 (buffer A). Before and after freezing, the oxygen-evolution activity assessed at 28 °C in the presence of 1 M glycine betaine had been 1200–1400 μmol O_2 per mg Chl and hour. Before use the samples were thawed for at least 1 h on ice and washed by dilution in buffer A and centrifugation. The resulting pellet was resuspended in buffer A to a Chl concentration of 10 μg/mL and stored on ice until use. For measurement of the pH-dependence, the pellet was resuspended in a buffer containing 10% glycerol, 1 M glycine betaine, 25 mM MES, 25 mM MOPS, 25 mM EPPS, 10 mM NaCl, 5 mM $MgCl_2$ and 5 mM $CaCl_2$; the pH was adjusted by addition of HCl and NaOH. One minute before the measurement, the electron acceptor DCBQ was added to yield a concentration of 20 μM. The addition of DCBQ caused a slight fluorescence quenching (20% at the F_0-level; 40% at the F_M-level).

2.2. Time-resolved measurements of delayed Chl fluorescence

In the delayed fluorescence experiment, the dark-adapted samples were excited by a saturating Laser flash of 2 mJ/cm^2 (Continuum Minilite II, $\lambda = 532$ nm, fwhm of 5 ns, time between flashes of 0.7 s). The Laser beam was widened by lenses and shaped by an aperture to yield approximately homogenous illumination of a quadratic area of 1 cm^2 matching the width of the used optical cuvette. Pulse intensities were determined using a Nova-Laser-Power/Energy-Monitor, measuring head PE10 (Ophir Optronics).

To avoid saturation of the detector system caused by the strong prompt fluorescence of the probe during laser excitation, a gated photomultiplier was used (Hamamatsu R2066; PMT Gated Socket Assembly C1392-55; anode voltage, 1000V ; anode resistor, 2.2 kΩ, gating voltage, 240 V applied from 7 μs before to 3 μs after the Laser flash). Scattered Laser light was blocked by a combination of two long-pass filters (LINOS Photonics, DT-red and DT-magenta with cut-off wavelengths of 600 and 632 nm, respectively). After amplification (Tektronix AM502, chosen low-pass bandwidth of 300 kHz) the signal was sampled at 1 MHz by a 12 bit PC-card (ADLINK, PCI 9812) for 200 ms before and 56 ms after the Laser flash. Starting at 10 μs after each Laser flash, to reduce the number of data points and the noise level, following AD-conversion the data point were averaged within an exponentially increasing time interval such that the ratio of the lengths of two neighboring time intervals was a constant value (c_{avg}). The averaging was done immediately after measurement of the DF decay by a home-made computer program. The value of c_{avg} was chosen such that in the time domain 18 points per decade were obtained. For presentation on a logarithmic time axis, this averaging procedure leads to a constant spacing of the resulting data points (therefore in the following denoted as logarithmic averaging). The intensity of the delayed fluorescence decreases by about five orders of magnitude in the time range from 10 μs to 60 ms after the laser flash. By virtue of the logarithmic averaging the relative noise level (measured in percent of the actual signal) was comparable over the complete time range.

The extreme dynamic range of the delayed fluorescence signal (decrease of the signal by a factor 10^4 to 10^6 from 10 μs to 60 ms) renders the 12-bit resolution of the AD converter critical. Therefore the following approach was chosen. The voltage at the PM anode resistor was branched and fed in two parallel chains of amplifiers. In the first branch, the signal was directly fed into the Tektronix amplifier (Tektronix AM 502). In the second branch, the PM signal was amplified by a factor of 30 (home-built amplifier, bandwidth of 1.5 MHz) and then fed into a second Tektronix amplifier (Tektronix AM 502, low-pass bandwidth of 300 kHz). The output signals of the two Tektronix amplifiers were separately converted to a digital signal. The signal of the second branch exceeded the input-voltage range of the AD converter within the first 400 μs after the flash (overload), the signal of the first branch was in the ms time domain below the resolution limit of the AD converter. After logarithmic averaging of the signals of both branches, the two signals were combined by appropriate scaling of the signal of the second branch. Eventually the first branch provided the data points for $t < 500$ μs and the second branch the data points for $t > 500$ μs.

The data were corrected for an artefact of the detection system which predominantly results from excitation of delayed fluorescence in the glass or cathode material of the photomultiplier by the strong prompt fluorescence of the PSII particles as well as by scattered light of the excitation flash. The details of the correction procedure are described elsewhere [14].

2.3. Time-resolved measurements of prompt Chl fluorescence

For prompt fluorescence measurements, the samples were excited with ns Laser pulses (pump pulse) as described above. The time courses in the yield of the prompt fluorescence [10] were measured using a pump-probe technique with logarithmically spaced probe pulses (6 pulses per decade, 100 μs to 690 ms). A commercially available instrument was used for probe-pulse generation and fluorescence detection (FL 3000, Photo Systems Instruments). Probe pulses of 5 μs duration were provided by two arrays with seven LEDs each ($\lambda_{max} = 615$ nm, HLMP-DH08, Hewlett Packard). The ns-laser excited the sample via the open topside of the cuvette. A PIN photodiode was used for detection at right angle to the exciting laser pulse and the LED probe pulses.

For delayed and prompt fluorescence measurements, the temperature of the sample was controlled using a combination of water bath and circulator (Haake, DC50) and a laboratory built water-jacketed cuvette holder. We estimate the imprecision in the sample temperature to be smaller than ±1 °C.

2.4. Curve-fitting

The detected time courses were simulated using a sum of exponential functions:

$$F(t) = \left(\sum_{i=1}^{3} a_i \exp(-t/\tau_i) \right) + c.$$

The parameters a_i, c, and τ_i were determined by minimization of the error sum. For simulation of the prompt fluorescence, a conventional least-square fit was carried out. For curve-fitting of the logarithmically averaged delayed fluorescence decays, the error sum was calculated according to:

$$\varepsilon^2 = \sum_{N} \left(\log \frac{F_{sim}}{F_{exp}} \right)^2.$$

The ‘mean time constant’ and Gibbs free-energy of intermediate formation in the $S_3 \rightarrow S_0$ were calculated according to:

$$\tau_{mean} = \frac{\sum_i a_i \tau_i}{\sum_i a_i}$$

and

$$\Delta G = -k_B T \ln \frac{\sum_i a_i + c}{a_{slow} + c}$$

respectively, where the sum includes all exponential components used to model the multiphasic process of intermediate formation.

The prompt fluorescence decays ($F_P(t)$) were simulated using three exponentials and the continuous function obtained from the fit was used for the Q_A^--decay correction of $F_D(t)$ as described further below.

3. Results and discussion

3.1. Rationale for analysis of DF decay curves

In the following the origin of the delayed chlorophyll fluorescence as well as the rationale for the analysis of the DF time courses is outlined. Delayed fluorescence emission (or luminescence) of chloroplasts, which is delayed (>20 ns after the photon absorption event) with respect to the prompt fluorescence (<20 ns), has been discovered by Strehler and Arnold [29] and has been repeatedly employed as a tool in photosynthesis research (see, e.g., [30–35]).

The delayed fluorescence of PSII is emitted by the bulk of the PSII antenna chlorophylls as suggested by the comparison of the spectra of prompt and delayed chlorophyll fluorescence (for recent precision measurements, see [14,36]). The essentially perfect identity of the spectra indicates that prompt and delayed fluorescence originate from the same excited state of the PSII antenna system (Chl*-state), which is characterized by an equilibrium distribution of excited states among the PSII antenna chlorophylls (rapid exciton equilibration; see, e.g. [10,11]). The delayed fluorescence (DF) results from repopulation of the Chl*-state of the PSII antenna system by recombination of radical-pair states. Once the Chl*-state is repopulated, either (i) the primary and secondary radical-pair states are formed once again or (ii) the excited state decays thermally or (iii) it decays by emission of a fluorescence photon. The latter path gives rise to fluorescence emission which is delayed with respect to the initial photon-absorption events by clearly more than the excited-state lifetime. The emission of the fluorescence photon may be delayed by microseconds, milliseconds or even seconds.

The DF intensity and its temporal changes after excitation by a short light pulse are best understood in terms of an equilibrium consideration. (An equilibrium approach is applicable because the influence of loss processes on the populations is, to a first approximation, negligible, as discussed elsewhere [14].) For an ensemble of PSII, the actual population of the Chl*-state (fraction of PSII in the Chl*-state denoted as [Chl*]) is assumed to be determined by the free-energy difference between the excited-antenna state and the radical-pair state reached at this time according to

$$\frac{[\mathrm{Chl}^*]}{[\mathrm{RP}]} = e^{\Delta G^*_{RP}/k_B T}, \tag{1}$$

where ΔG^*_{RP} represent the difference in Gibbs' free energy ($\Delta G^*_{RP}<0$) between the excited-antenna state (Chl*) and the radical-pair state (RP), k_B is the Boltzmann constant, and T is the absolute temperature in Kelvin. Consequently the DF intensity is given by

$$F_D = S[\mathrm{Chl}^*] = S[\mathrm{RP}]e^{\Delta G^*_{RP}/k_B T}, \tag{2}$$

or for [RP] ≈ 1,

$$F_D = S e^{\Delta G^*_{RP}/k_B T}, \tag{3}$$

where S is a time-independent factor which is determined by the value of the rate constant for fluorescence emission of the antenna chlorophylls [14].

After flash-excitation the DF of PSII decreases rapidly. A decrease in the fluorescence intensity is explainable by the transition from a first radical-pair state (RP1) to a second radical-pair state (RP2) with ΔG^*_{RP2} being more negative than ΔG^*_{RP1}. Consequently the DF intensity decreases in the course of this transition from $F_D^{initial}$, a value which is determined by ΔG^*_{RP1}, to F_D^{final}, a value which is determined by ΔG^*_{RP2}. For the ratio of the F_D-levels it is obtained:

$$\frac{F_D^{initial}}{F_D^{final}} = \frac{e^{\Delta G^*_{RP1}/k_B T}}{e^{\Delta G^*_{RP2}/k_B T}} = e^{(\Delta G^*_{RP1} - \Delta G^*_{RP2})/k_B T} \tag{4}$$

Thus, for a kinetically resolvable downhill transition between two radical-pair states the associated difference in Gibbs' free energy can be determined according to Eq. (4). The fluorescence decay from $F_C^{initial}$ to F_D^{final} reflects the time course of the transition between the two states and can be used to determine rate-constant values.

Frequently also an alternative description of the DF intensity of PSII is useful: At any time, the delayed fluorescence intensity is determined, to a good approximation, by the fraction of PSII with reduced Q_A (denoted as $[Q_A^-]$) and by the fraction of PSII with oxidized P680 (denoted as $[P680^+]$) according to:

$$F_D(t) = \mathrm{S} e^{\Delta G^*/k_B T}[P680^+](t)[Q_A^-](t), \tag{5}$$

where ΔG^* is the free energy difference between the excited-antenna state and the ($P680^+$, Q_A^-) radical pair. For formation of a distinct radical pair in the majority of the PSII, the above equation is fully equivalent to Eq. (3). For example, in the presence of the (Q_A^-, $Y_Z^{\bullet+}$) radical-pair state the $P680^+$-state is populated according to:

$$[\mathrm{P680}^+] = [Y_Z^{\bullet+}] e^{\Delta G_{P680-YZ}/k_B T}, \tag{6}$$

where $\Delta G_{P680\text{-}YZ}$ is the free-energy associated with formation of the $Y_Z^{\bullet+}$-state. Assuming that Q_A^- and $Y_Z^{\bullet+}$ have been formed in the majority of the PSII, we obtain the following relation

$$\begin{aligned} F_D &= S e^{\Delta G^*/k_B T}[Y_Z^{\bullet+}][Q_A^-] e^{\Delta G_{P680-YZ}/k_B T} \\ &= \mathrm{S} e^{(\Delta G^* + \Delta G_{P680-YZ})/k_B T}. \end{aligned} \tag{7}$$

Comparison of the above equation with Eq. (2) illustrates that the Eqs. (3) and (5) represent an equivalent description.

(The general proof of the equivalence of Eqs. (3) and (5) is straightforward and therefore not presented.)

3.2. Measurement and analysis of DF decay curves

For a sequence of Laser flashes, time courses of the delayed fluorescence intensity were measured. The time window used in the present work extends from 10 μs to 10 ms after the Laser flash; typical time courses are shown in Fig. 3.

A clear period-of-four pattern is visible in the time courses demonstrating that the reactions at the PSII donor-side reactions determine the delayed-fluorescence decays. After the third flash, a clear millisecond phase is visible (Fig. 3B). Its flash-number dependence (Fig. 3C) and time constant (Fig. 3D) facilitates assignment to the simultaneous events of (i) electron transfer from the Mn complex to $Y_Z^{\bullet}$ and (ii) dioxygen formation in the $S_4 \rightarrow S_0$ transition.

We note that at all times the delayed fluorescence induced by the first and second flash is clearly smaller than the third-flash signal (Figs. 3A and B). Therefore, a correction of the third-flash signal for the contribution by the minority fraction of PSII (around 20%) that undergoes the $S_2 \rightarrow S_3$ transition not on the second, but on the third flash (due to 'misses' on the first or second flash) is not required. In the following we focus on the third-flash time

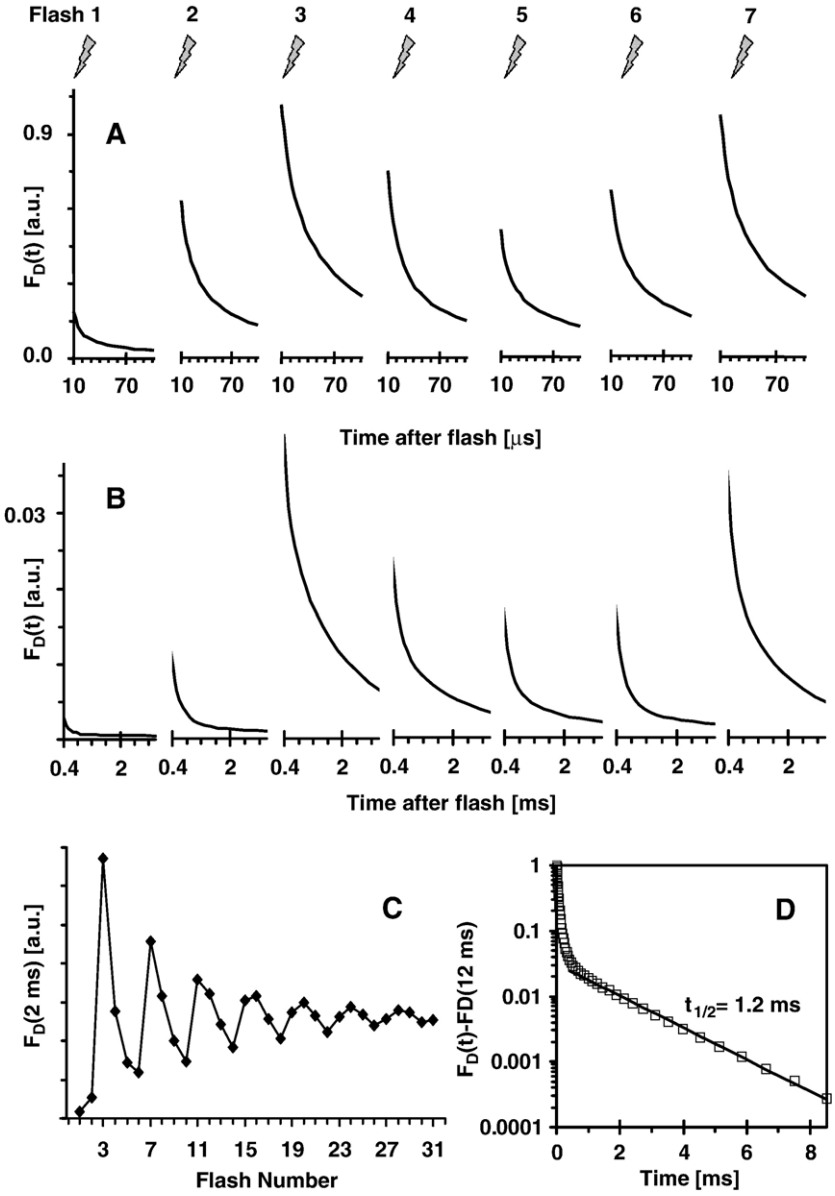

Fig. 3. Time course of delayed fluorescence for the first seven flashes applied to dark-adapted PSII particles (A and B), flash-number dependence of magnitude of millisecond phase (C) and semi-logarithmic plot of millisecond phase (D). In A and B, the DF time courses induced by a train of saturating ns-laser flashes are shown for a time period after the respective flash of 10 to 100 μs (A) and 400 μs to 3 ms (B) (pH 6.4, 20 °C). As shown in C, the delayed fluorescence detected at 2 ms after the flash shows the typical flash-number dependence of dioxygen formation first reported by Joliot [37] and Kok [15]. In D, the semi-logarithmic plot of the third-flash decay demonstrates the mono-exponential phase of dioxygen formation with a halftime of ~1.2 ms.

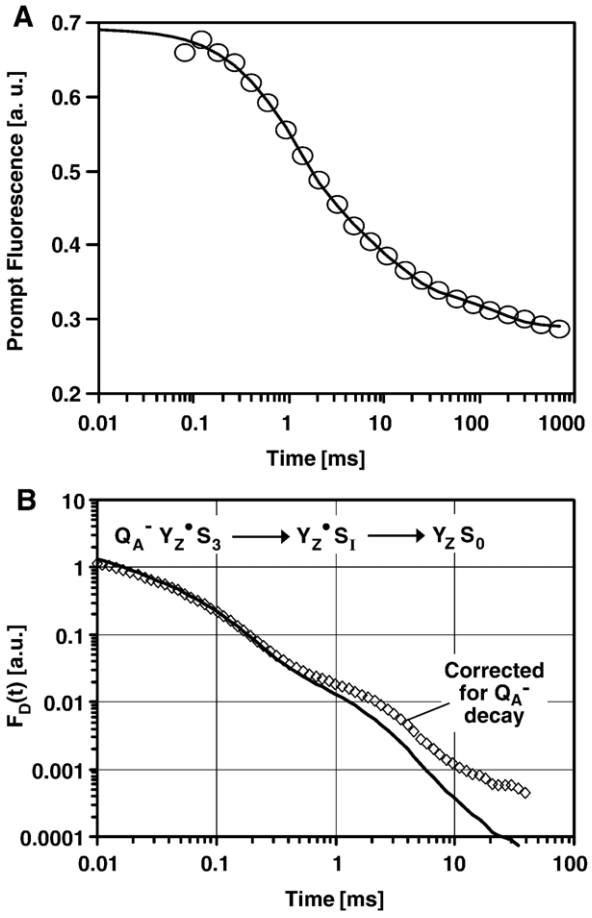

Fig. 4. (A) Changes in the yield of prompt fluorescence and (B) delayed fluorescence decay without and with correction for the influence of the Q_A reoxidation. The time courses were detected after the third laser-flash applied to dark-adapted PSII particles (pH 6.4, 20 °C). (A) The changes in the yield of the prompt fluorescence (unfilled circles) were measured in a pump-probe experiment as described in Materials and methods. The solid line was obtained by a tri-exponential simulation. (B) The delayed fluorescence decays are shown before (line) and after correction (diamonds) for the influence of changes in the fraction of PSII with reduced Q_A. The delayed fluorescence data were corrected according to Eq. (8) using the $F_P(t)$ obtained by the tri-exponential simulation of the prompt fluorescence. We note that the y-scale in A is linear whereas it is logarithmic in B. In B also indicated is the assignment to S-states of the initial plateau level (S_3), of the intermediate plateau (S_1 or S_4) and of the final level (S_0).

courses, which are directly related to the kinetics and energetics of dioxygen formation in the $S_3 \rightarrow S_4 \rightarrow S_0$ transition.

Recently it has been shown [9] that dioxygen formation is preceded by a process which is completed within about 200 μs and tentatively has been assigned to the formation of an S_4-state by a deprotonation process (see Introduction). In the delayed fluorescence transients the formation of an intermediate state prior to the onset of dioxygen formation is clearly visible (Fig. 4). Within less than 1 μs after the Laser flash the Y_Z is oxidized by electron transfer to P680. Subsequently the S_4-state is formed. This S_4-state formation relates to a drop in the intensity of the delayed fluorescence by a factor of almost hundred, as clearly visible in Figs. 4 and 5.

According to Eq. (5), the DF intensity decreases due to a decay of $[P680^+]$ or of $[Q_A^-]$. We find (see below) that in the time range from 10 μs to 10 ms, $F_D(t)$ changes by more than three orders of magnitude whereas the concentration of Q_A^- changes only by a factor of about four (neglecting the non-linearity in the relation between the prompt-fluorescence-yield and the Q_A^- concentration [10,38], which is of minor influence in the used PSII membrane particles [14]). This means that the delayed-fluorescence decay is predominantly determined by $[P680^+](t)$, i.e. the population of the $P680^+$ state. The Q_A^- influence is small, but is not fully negligible, especially for $t > 300$ μs (as shown below).

(We note that, in Fig. 4A, the decrease in the prompt fluorescence by a factor of four within 10 ms after laser-flash application is *not* indicative of a halftime of the Q_A–Q_B electron transfer of ~5 ms. The changes in the Q_A^- concentration

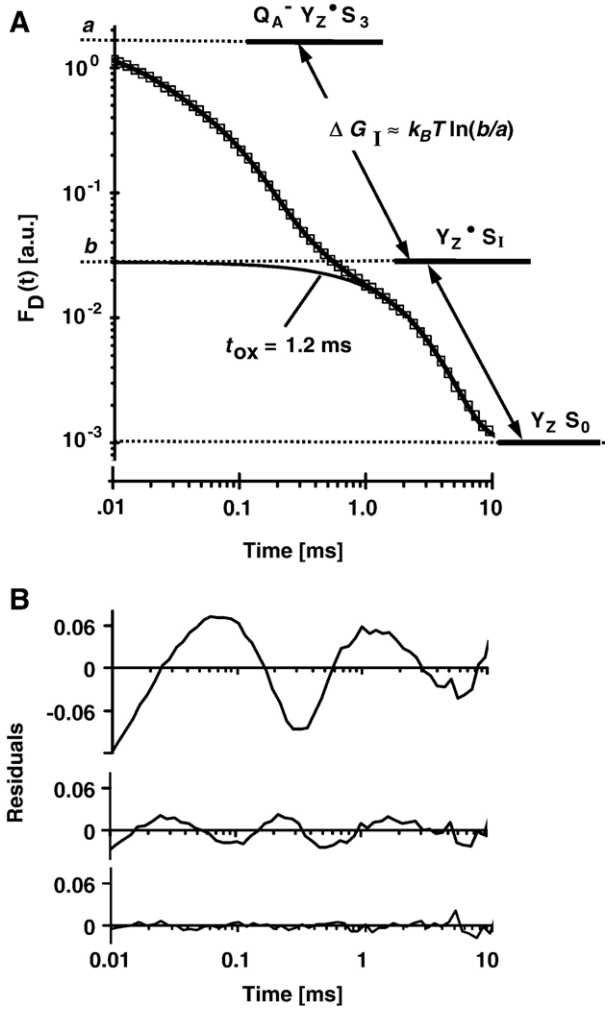

Fig. 5. Simulation of the delayed fluorescence decay after the third flash by a sum of exponentials. (A) Q_A-corrected delayed fluorescence decay (squares; pH 6.4, 20 °C) and simulation with a sum of three decaying exponential functions (line) are shown in combination with a scheme of the corresponding PSII states. The contribution of the dioxygen-formation phase with a halftime of ~1.2 ms is shown as a separate line. The dotted lines labels by 'a' and 'b' indicate the levels used for calculation of ΔG_I. (B) Residual plots for simulation of the delayed fluorescence decays with a sum of two exponentials (top trace in B; time constants of 67 μs and 1.6 ms), three exponentials (intermediate trace; 27 μs, 114 μs, 1.8 ms) and four exponentials (bottom trace; 14 μs, 65 μs, 203 μs, 1.9 ms) (Residuals equals log(Simulation/Experiment)).

after flash excitation are multiphasic with sizable slow contributions likely explainable by changes in the occupancy of the Q_B-site [39]. Furthermore, the apparent halftimes of 1.8 ms in Fig. 4A were considerably longer [40] than those in thylakoids from plant material [39,41–43] and in the non-oxygenic, but structurally related reaction center of purple bacteria [44,45]; an effect of the detergent on the quinone-reducing side of PSII cannot be excluded.)

On the basis of Eq. (5), a correction for the $[Q_A^-]$-decay contribution to DF time courses is approached. Therefore the changes in $[Q_A^-]$ were assessed by analysis of $F_P(t)$, the time course of the yield of the prompt Chl fluorescence (Fig. 4A). The time-dependent fluorescence yield was measured by application of a sequence of weak probe pulses (provided by light-emitting diodes) which were applied at distinct time after the saturating Laser flash (see Materials and methods). The relation between $F_P(t)$ and fraction of PSII with reduced Q_A is well established (for review see [10]) so that a correction of $F_D(t)$ for the decrease in the Q_A^- concentration is straightforward. On the basis of Eq. (5), the corrected values of $F_D(t)$ are calculated according to:

$$F_D^{corr}(t) = F_D(t)\left(\frac{F_M - F_0}{F_p(t) - F_0}\right), \quad (8)$$

where F_M is the maximum and F_o the minimum level of prompt fluorescence.

This correction amounts to a division of the expression for $F_D(t)$ given in Eq. (5) by $[Q_A^-](t)$, the concentration of PSII with reduced Q_A. In addition the correction eliminates the possible influence of PSII connectivity on $F_D^{corr}(t)$, as shown elsewhere [46].

Thus,

$$F_D^{corr}(t) \approx S' e^{\Delta G^*/k_B T}[P680^+](t). \quad (9)$$

Fig. 4B shows the original and the Q_A-corrected time course of the delayed fluorescence. Significant deviations are visible for $t > 300$ μs but, as shown further below, the kinetic parameters of interest are only marginally affected by this correction (see also [13,47–49]). For increased precision in the kinetic parameters, in the following only corrected times courses are analyzed. For simplicity, the superscript 'corr' is dropped in the following.

Visual inspection of the corrected delayed-fluorescence decays in Figs. 4B and 5A immediately reveals the principally biphasic behavior. Starting at a plateau level at $t < 10$ μs the delayed fluorescence declines up to second plateau level at ~0.5 ms after the flash which is followed by the final decline characterized by a halftime of ~1.2 ms. As discussed above, the first decay phase is assignable to the intermediate formation (S_4 in Fig. 1) which occurs before the eventual dioxygen formation, which is associated with the millisecond phase.

The corrected $F_D(t)$ was simulated by a sum of exponential functions (curve-fitting). A bi-exponential fit was unacceptable (top trace in Fig. 5B). For a tri-exponential fit the simulated and experimental curve match reasonably well (middle trace in Fig. 5B, compare also solid line and squares in Fig. 5A), but excellent agreement was obtained only for simulation by a sum of four exponentials. Whereas the millisecond phase is very well described by a single exponential (see Figs. 3D and 5A), the process of S_4-formation clearly is multiphasic. Three exponential functions are required for its description suggesting that at least three, (presumably) sequential reaction steps are involved in formation of the S_4-intermediate. Since there may be more than three steps involved, determination of the individual rate constants of the multiphasic reaction step is problematic. For calculation of the free-energy change associated with S_4-formation, however, only the total amplitude of the first decay phase is required. Its value corresponds to the sum of the individual amplitudes (pre-exponential factors) and does not critically depend on the used simulation approach. To avoid any underdetermined fits, in the following a tri-exponential simulation is used (two exponentials for intermediate formation plus single exponential for dioxygen formation).

In [50], we have compared the DF transients, on the one hand, with the time courses of the X-ray signals which reflect the Mn oxidation state, on the other hand. Therefore it was assumed that three sequential reaction steps precede the onset of Mn reduction in the dioxygen-formation step [18]. The rate constants of these sequential steps were derived from a tri-exponential fit of the $S_3 \rightarrow S_4$ phase in the DF transients (k_i^{-1} equal to 14 μs, 65 μs, and 203 μs). Thereby good agreement between simulated and measured X-ray time courses was obtained. A model of two or three parallel reactions could not reproduce the experimentally observed lag phase in the X-ray transients; assuming two sequential steps preceding dioxygen formation, the agreement was not satisfactorily (bi-exponential fit of $S_3 \rightarrow S_4$ phase in the DF transients, k_i^{-1} equal to 27 μs and 114 μs). Nonetheless, in the following a bi-exponential fit of the S_4-formation phase is employed since this approach (i) ensures highly reproducible fit parameters and (ii) is sufficiently accurate for determination of the free-energy difference associated with the $S_3 \rightarrow S_4$ transition.

The fit results were used to determine three kinetic (or thermodynamic) parameters (Table 1). The value of the dioxygen-formation rate constant resulted directly from the fits (reciprocal value of the slowest time constant). The difference in the Gibbs' free energy associated with the $S_3 \rightarrow S_4$ transition as well as its mean time constant were directly calculated from the simulation

Table 1
Kinetic parameters derived for the $S_3 \rightarrow S_4 \rightarrow S_0$ transition

	Uncorrected	Q_A correction
$S_3 \rightarrow S_4$, τ_{mean} [μs]	91±3	98±4
$S_3 \rightarrow S_4$, ΔG [meV]	−97±1	−92±1
$S_4 \rightarrow S_0$, τ_{ox} [ms]	1.43±0.04	1.64±0.04

The time constants and the free-energy difference were determined by simulation of delayed-fluorescence time courses measured on suspensions of PSII membrane particles at pH 6.4 and 19.5 °C. In the third column, the DF decays were corrected for the influence of the decrease in the concentration of reduced Q_A. The given error ranges represent the standard deviation in the parameters (4 data sets). We note that the value of τ_{mean} was calculated according to the equation for the mean time constant given in Curve fitting; it differs from the time-constants of the slowest reaction steps in S_4-formation.

parameters by the equations given in Materials and methods. We note that the S_4-formation is associated with a sizable free-energy change of −92 meV (−8.9 kJ/mol or −2.1 kcal/mol).

We also assessed the influence of the correction for the Q_A^- decay on the simulation results. Comparison of the second and third row in Table 1 reveals that parameters resulting from simulation of uncorrected DF time courses are relatively close to the ones determined for the corrected time courses. The corresponding comparison for DF transients collected at other temperatures confirmed this observation (data not shown). Even though the difference is small, in the following we refer exclusively to simulation results obtained for time courses which have been corrected for the Q_A^- decay.

We note that the correction for Q_A^- oxidation does not exclude *per se* any acceptor-side influence. Changes at the acceptor side might affect the ΔG^*-value in Eq. (5). For example, a protonation at the acceptor side induced by Q_A^- formation might result in a shift of the Q_A^- potential and thus affect ΔG^*. The period-four pattern suggests that the donor side influence on the DF transients is dominating and the characteristics of the sub-ms phase in the delayed fluorescence suggests assignment to a donor-side deprotonation process ([9,14], unpublished results). To corroborate further that the investigated intermediate formation is a donor side process, the time dependence of the $P680^+$ concentration was assessed. In the case of a pure donor side process, the $P680^+$ time course should reflect the time course of the delayed chlorophyll fluorescence (Eq. (3)). For verification the $P680^+$ concentration was assessed by exploiting its capacity to quench the prompt chlorophyll fluorescence. (This method was chosen because suspensions of PSII membrane particles strongly scatter light so that measurements of the absorption changes associated with $P680^+$ formation are problematic.) The thus obtained results confirm that the delayed fluorescence time courses reflect the concentration of $P680^+$ (data not shown, see [46]).

3.3. Activation energy of dioxygen formation step

The DF analysis was applied for determination of the temperature dependence of the dioxygen-formation rate constant. In [27] and [51] the temperature dependence was investigated and activation energies of 340 meV (UV data in [27]), 420 meV (polarographic data [27]), and 380 meV [52], respectively, have been determined. In [26] the Arrhenius plot revealed a breakpoint at 6 °C and activation energies of 208 meV and 477 meV were determined for $T>6$ °C and $T<6$ °C, respectively. In [26] the lowest temperature used for measurements had been 0 °C and due to the low number of data points, the visual inspection of the data did not allow for an estimate of the scatter in the data and the reproducibility in the measurements. In the present study we extended the investigated range to −2.7 °C by using 10% glycerol for lowering of the freezing point of the sample.

Sixty time courses were measured at temperatures ranging from −2.7 °C to 27.5 °C and analyzed as described above. The rate-constant values determined by curve-fitting of the third-flash transients are shown in Fig. 6 in form of an Arrhenius plot. The Arrhenius plot can be interpreted in two ways. In Fig. 6A two lines are drawn which correspond to two different activation energies, namely $E_a=182$ meV for $T>15$ °C and $E_a=257$ meV for $T<6$ °C. Visual inspection reveals that, rather than having a distinct breakpoint temperature, a continuous transition between the low-E_a ($T>15$ °C) and high-E_a ($T<6$ °C) regime might be involved. However, the putative breakpoint behavior is emphasized by the graphical presentation in Fig. 6A and not easily identified without this suggestive presentation. In Fig. 6B a single activation energy of 231 meV was assumed (solid line) and a reasonably good description for the complete temperature range is obtained. The calculated activation energy value is in reasonably good agreement with the above mentioned values of [26] for $T>6$ °C. (The activation energy determined in [27] and [51] were significantly greater than in the present study. Differences in the buffer composition, species or type of preparation might play a role.) We did not observe an activation energy for $T<6$ °C which is as high as the value 477 meV reported in [26]. In conclusion, we cannot exclude the occurrence of a breakpoint in the temperature dependence of the rate constant of dioxygen formation. However, to a good approximation the data is describable already by a simple monophasic Arrhenius behavior. Also by polarographic measurements of dioxygen formation on cyanobacterial PSII membranes (*Synechocystis* species), a breakpoint in the Arrhenius

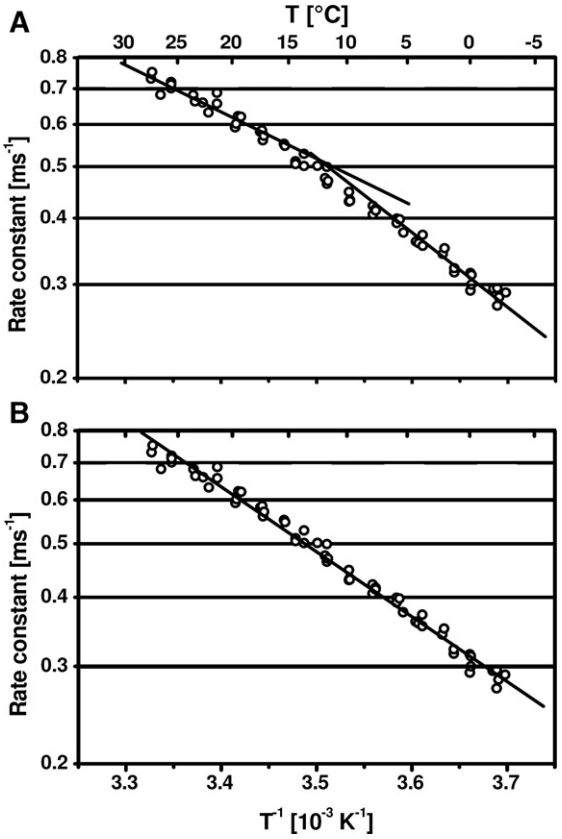

Fig. 6. Temperature dependence of the rate constant for dioxygen formation. The open circles represent the rate constant values as determined by analysis of DF decays. The straight lines in A correspond to activation energies of 257 meV (determined for $T<6$ °C) and 182 meV (determined for $T>15$ °C). In B, the straight line corresponds to a single activation energy of 231 meV (the data points in A and B are identical).

plot was *not* detectable [27]. Extension of the temperature range or studies on PSII of thermophilic cyanobacteria [53] might facilitate an unambiguous identification of a temperature-dependent switch between two distinct activation energies.

3.4. Conclusions

(1) The delayed fluorescence (DF) emission of PSII is a useful tool to study quantitatively light-induced electron transfer and related processes (e.g., proton movements) which are associated with a free-energy drop. In the here investigated time domain, the DF decays are dominated by processes at the donor side of PSII. A correction for the acceptor-side contribution which results from the decrease in the number of PSII with reduced Q_A is proposed (Eq. (8)). This correction requires time-resolved measurements of the variable yield of the prompt Chl fluorescence. There are no indications for further acceptor-side contributions to the DF time courses.

(2) Quantitative analysis of the DF transients facilitates determination of free-energy changes and rate constants. The underlying rationale is straightforward (described in the context of Eqs. (1)–(7). The quantitative analysis itself is found to be straightforward only for the DF transients induced by the third flash because the formation of (i) an intermediate state and (ii) the O–O bond formation step are kinetically well resolvable. For the transients induced by the first, second and fourth flash the quantitative analysis is clearly more demanding (work in progress). We note in passing that also a sizable fraction of PSII with a defect donor side might seriously complicate the analysis.

(3) The DF transients induced by the third flash applied to dark-adapted PSII reflect the kinetically resolvable steps of dioxygen formation in the $S_3 \rightarrow S_0$ transition. We find that the recently reported formation of an S_4-intermediate prior to the onset of O–O bond formation [9] is a multiphasic process involving three or more steps, as anticipated for proton movements from the manganese complex of PSII to the aqueous bulk phase. (Since typical distances for proton tunneling are clearly below 1.5 Å, the actual proton movement along the path suggested in [3,54] will require, at the atomic level, much more than three proton-transfer steps. However, only three of these steps were kinetically resolvable in the DF experiment.) At pH 6.4 and 19.5 °C, the slowest reaction step in S_4-formation is characterized by a time constant of ~200 μs, the mean time constant is ~100 μs (calculated as described in Curve fitting), and the free-energy difference associated with the $S_3 \rightarrow S_4$ transition exceeds 90 meV.

(4) The temperature dependence of the rate constant of dioxygen formation was investigated ($T = -2.7$ to 27.5 °C) and a value of 231 meV is determined for the approximately temperature-independent activation energy. There are weak indications for a biphasicity in the Arrhenius plot, but clear-cut evidence for a temperature-dependent switch between two activation energies is not obtained.

Elucidation of the events involved in S_4-formation and the proposed relation to deprotonation events [9,16–18,55] requires further investigations. The described DF approach may play a prominent role in these and other studies on photosynthetic water oxidation.

Acknowledgements

We thank Monika Fünning for the skilled preparation of PSII membrane particles, and Dr. Michael Haumann for his support and stimulating discussions on the subject of the present work. Financial support by the Bundesministerium für Bildung und Forschung (BMBF 03SF0318C) in the research consortium "Grundlagen für einen biotechnologischen und biomimetischen Ansatz der Wasserstoffproduktion" and by the Deutsche Forschungsgemeinschaft (project C6 in the SFB 498) is gratefully acknowledged.

References

[1] A. Zouni, H.T. Witt, J. Kern, P. Fromme, N. Krauss, W. Saenger, P. Orth, Crystal structure of photosystem II from *Synechococcus elongatus* at 3.8 Å resolution, Nature 409 (2001) 739–743.
[2] N. Kamiya, J.-R. Shen, Crystal structure of oxygen-evolving photosystem II from *Thermosynechococcus vulcanus* at 3.7-Å resolution, Proc. Natl. Acad. Sci. U. S. A. 100 (2003) 98–103.
[3] K.N. Ferreira, T.M. Iverson, K. Maghlaoui, J. Barber, S. Iwata, Architecture of the photosynthetic oxygen-evolving center, Science 303 (2004) 1831–1838.
[4] B. Loll, J. Kern, W. Saenger, A. Zouni, J. Biesiadka, Towards complete cofactor arrangement in the 3.0 A resolution structure of photosystem II, Nature 438 (2005) 1040–1044.
[5] M. Haumann, P. Pospisil, M. Grabolle, C. Muller, P. Liebisch, V.A. Sole, T. Neisius, J. Dittmer, L. Iuzzolino, H. Dau, First steps towards time-resolved BioXAS at room temperature: state transitions of the manganese complex of oxygenic photosynthesis, J. Synchrotron Radiat. 9 (2002) 304–308.
[6] M. Haumann, C. Müller, P. Liebisch, T. Neisius, H. Dau, A novel BioXAS technique with sub-millisecond time resolution to track oxidation state and structural changes at biological metal centers, J. Synchrotron Radiat. 12 (2005) 35–44.
[7] M. Haumann, C. Müller, P. Liebisch, L. Iuzzolino, J. Dittmer, M. Grabolle, T. Neisius, W. Meyer-Klaucke, H. Dau, Structural and oxidation state changes of the photosystem II manganese complex in four transitions of the water oxidation cycle ($S_0 \rightarrow S_1$, $S_1 \rightarrow S_2$, $S_2 \rightarrow S_3$, $S_{3,4} \rightarrow S_0$) characterized by X-ray absorption spectroscopy at 20 K as well as at room temperature, Biochemistry 44 (2005) 1894–1908.
[8] H. Dau, M. Haumann, X-ray absorption spectroscopy to watch catalysis by metalloenzymes: status and perspectives discussed for the water-splitting manganese complex of photosynthesis, J. Synchrotron Radiat. 10 (2003) 76–85.
[9] M. Haumann, P. Liebisch, C. Müller, M. Barra, M. Grabolle, H. Dau, Photosynthetic O_2 formation tracked by time-resolved X-ray experiments, Science 310 (2005) 1019–1021.
[10] H. Dau, Molecular mechanisms and quantitative models of variable photosystem II fluorescence, Photochem. Photobiol. 60 (1994) 1–23.
[11] H. Dau, K. Sauer, Exciton equilibration and photosystem II exciton dynamics — a fluorescence study on photosystem II membrane particles of spinach, Biochim. Biophys. Acta 1273 (1996) 175–190.
[12] J. Clausen, W. Junge, Detection of an intermediate of photosynthetic water oxidation, Nature 430 (2004) 480–483.
[13] J. Clausen, W. Junge, H. Dau, M. Haumann, Photosynthetic water oxidation at high O_2 backpressure monitored by delayed chlorophyll fluorescence, Biochemistry 44 (2005) 12775–12779.
[14] M. Grabolle, H. Dau, Energetics of primary and secondary electron transfer in Photosystem II membrane particles of spinach revisited on basis of

recombination-fluorescence measurements, Biochim. Biophys. Acta 1708 (2005) 209–218.
[15] B. Kok, B. Forbush, M. McGloin, Cooperation of charges in photosynthetic O2 evolution — I, Photochem. Photobiol. 11 (1970) 457–475.
[16] H. Dau, M. Haumann, Reaction cycle of photosynthetic water oxidation in plants and cyanobacteria, Science 312 (2006) 1471–1472.
[17] H. Dau, M. Haumann, Eight steps preceding O–O bond formation in oxygenic photosynthesis —a basic reaction cycle of the Photosystem II manganese complex, Biochim. Biophys. Acta (2007-this issue), doi:10.1016/j.bbabio.2007.02.022.
[18] H. Dau, M. Haumann, Time-resolved X-ray spectroscopy leads to an extension of the classical S-state cycle model of photosynthetic oxygen evolution, Photosynth. Res. (in press).
[19] V.A. Shuvalov, F.F. Litvin, Mechanism of delayed light emission by plant leaves and of energy storage in photosynthesis centers, Mol. Biol. 3 (1969) 59–73.
[20] J. Lavorel, Kinetics of luminescence in the 10^{-6}–10^{-4}-s range in *Chlorella*, Biochim. Biophys. Acta 325 (1973) 213–229.
[21] J.M. Bowes, A.R. Crofts, Interactions of protons with transitions of the watersplitting enzyme of photosystem II as measured by delayed fluorescence, Z. Naturforsch. 33c (1978) 271–275.
[22] J.M. Bowes, A.R. Crofts, S. Itoh, Effects of pH on reactions on the donor side of photosystem II, Biochim. Biophys. Acta 547 (1979) 336–346.
[23] K. Zankel, Rapid delayed luminescence from chloroplasts: kinetic analysis of components; the relationship to the O_2 evolving system, Biochim. Biophys. Acta 245 (1971) 373–385.
[24] R. de Wijn, T. Schrama, H.J. van Gorkom, Secondary stabilization reactions and proton-coupled electron transport in photosystem II investigated by electroluminescence and fluorescence spectroscopy, Biochemistry 40 (2001) 5821–5834.
[25] J. Haveman, J. Lavorel, Identification of the 120 μs phase in the decay of delayed fluorescence in spinach chloroplasts and subchloroplast particles as the intrinsic back reaction. The dependence of the level of this phase on the thylakoids internal pH, Biochim. Biophys. Acta 408 (1975) 269–283.
[26] G. Renger, B. Hanssum, Studies on the reaction coordinates of the water oxidase in PS II membrane fragments from spinach, FEBS Lett. 299 (1992) 28–32.
[27] J. Clausen, R.J. Debus, W. Junge, Time-resolved oxygen production by PSII: chasing chemical intermediates, Biochim. Biophys. Acta 1655 (2004) 184–194.
[28] H. Schiller, H. Dau, Preparation protocols for high-activity Photosystem II membrane particles of green algae and higher plants, pH dependence of oxygen evolution and comparison of the S2-state multiline signal by X-band EPR spectroscopy, J. Photochem. Photobiol., B Biol. 55 (2000) 138–144.
[29] B. Strehler, W. Arnold, Light production by green plants, J. Gen. Physiol. 34 (1951) 809–820.
[30] K.L. Zankel, Rapid fluorescence changes observed in chloroplasts: their relationship to the O_2 evolving system, Biochim. Biophys. Acta 325 (1973) 138–148.
[31] K. Turzó, G. Laczkó, Z. Filus, P. Maróti, Quinone-dependent delayed fluorescence from the reaction center of photosynthetic bacteria, Biophys. J. 79 (2000) 14–25.
[32] R. de Wijn, T. Schrama, H.J. van Gorkom, Secondary stabilization reactions and proton-coupled electron transport in photosystem II investigated by electroluminescence and fluorescence spectroscopy, Biochemistry 40 (2001) 5821–5834.
[33] A.W. Rutherford, Govindjee, Y. Inoue, Charge accumulation and photochemistry in leaves studied by thermoluminescence and delayed light emission, Proc. Natl. Acad. Sci. U. S. A. 81 (1983) 1107–1111.
[34] I. Vass, G. Horvath, T. Herczeg, S. Demeter, Photosynthetic energy conservation investigated by thermoluminescence. Activation energies and half-lives of thermoluminescence bands of chloroplasts determined by mathematical resolution of glow curves, Biochim. Biophys. Acta 634 (1981) 140–152.
[35] I. Vass, Govindjee, Thermoluminescence from the photosynthetic apparatus, Photosynth. Res. 48 (1996) 117–126.
[36] A.D. Tsamaloukas, Fluoreszenzspektroskopie zur Excitonendynamik in den Chlorophyll-Antennen des Photosystems II der Pflanzen, Diploma thesis, FB Physik, FU Berlin (2001).
[37] P. Joliot, A. Joliot, Analysis of the interactions between the two photosystems in isolated chloroplasts, Biochim. Biophys. Acta 153 (1968) 635–652.
[38] J. Lavergne, H.W. Trissl, Theory of fluorescence induction in photosystem II: derivation of analytical expressions in a model including exciton-radical-pair equilibrium and restricted energy transfer between photosynthetic units, Biophys. J. 68 (1995) 2474–2492.
[39] R. de Wijn, H.J. van Gorkom, Kinetics of electron transfer from Q_a to Q_b in photosystem II, Biochemistry 40 (2001) 11912–11922.
[40] Putrenko II, S. Vasil'ev, S.D. Bruce, Modulation of flash-induced photosystem II fluorescence by events occurring at the water oxidizing complex, Biochemistry 38 (1999) 10632–10641.
[41] M. Haumann, W. Junge, The rates of proton uptake and electron transfer at the reducing side of photosystem II in thylakoids, FEBS Lett. 347 (1994) 45–50.
[42] A.R. Crofts, C.A. Wraight, The electrochemical domain of photosynthesis, Biochim. Biophys. Acta 726 (1983) 149–185.
[43] J.M. Bowes, A.R. Crofts, Binary oscillations in the rate of reoxidation of the primary acceptor of photosystem, Biochim. Biophys. Acta 590 (1980) 373–384.
[44] A. Remy, K. Gerwert, Coupling of light-induced electron transfer to proton uptake in photosynthesis, Nat. Struct. Biol. 10 (2003) 637–644.
[45] S. Hermes, O. Bremm, F. Garczarek, V. Derrien, P. Liebisch, P. Loja, P. Sebban, K. Gerwert, M. Haumann, A time-resolved iron-specific X-ray absorption experiment yields no evidence for an $Fe^{2+}\rightarrow Fe^{3+}$ transition during $Q_{A^-}\rightarrow Q_B$ electron transfer in the photosynthetic reaction center, Biochemistry 45 (2006) 353–359.
[46] M. Grabolle, Die Donorseite des Photosystems II: Rekombinationsfluoreszenz- und Röntgenabsorptionsstudien (thesis), Fachbereich Physik, Freie Univ. Berlin, http://www.diss.fu-berlin.de/2005/174/ (2005).
[47] M. Barra, M. Haumann, H. Dau, Specific loss of the extrinsic 18 KDa protein from photosystem II upon heating to 47 degrees C causes inactivation of oxygen evolution likely due to Ca release from the Mn-complex, Photosynth. Res. 84 (2005) 231–237.
[48] M. Barra, M. Haumann, P. Loja, R. Krivanek, A. Grundmeier, H. Dau, Intermediates in assembly by photoactivation after thermally accelerated disassembly of the manganese complex of photosynthetic water oxidation, Biochemistry 45 (2006) 14523–14532.
[49] M. Haumann, M. Barra, P. Loja, S. Löscher, R. Krivanek, A. Grundmeier, L.E. Andreasson, H. Dau, Bromide does not bind to the Mn_4Ca complex in its S_1 state in Cl^- depleted and Br^- reconstituted oxygen-evolving photosystem II: evidence from X-ray absorption spectroscopy at the Br K-edge, Biochemistry 45 (2006) 13101–13107.
[50] M. Haumann, P. Liebisch, C. Muller, M. Barra, M. Grabolle, H. Dau, Photosynthetic O2 formation tracked by time-resolved X-ray experiments, Science 310 (2005) 1019–1021.
[51] M. Haumann, O. Bögershausen, D. Cherepanov, R. Ahlbrink, W. Junge, Photosynthetic oxygen evolution: H/D isotope effects and the coupling between electron and proton transfer during the redox reactions at the oxidizing side of Photosystem, Photosynth. Res. 51 (1997) 193–208.
[52] M. Haumann, W. Junge, Extent and rate of proton release by photosynthetic water oxidation in thylakoids: electrostatic relaxation versus chemical production, Biochemistry 33 (1994) 864–872.
[53] H. Koike, B. Hanssum, Y. Inoue, G. Renger, Temperature dependence of S-state transition in a thermophilic cyanobacterium, *Synechococcus vulcanus* Copeland measured by absorption changes in the ultraviolet region, Biochim. Biophys. Acta 893 (1987) 524–533.
[54] H. Ishikita, W. Saenger, B. Loll, J. Biesiadka, E.W. Knapp, Energetics of a possible proton exit pathway for water oxidation in photosystem II, Biochemistry 45 (2006) 2063–2071.
[55] F. Rappaport, M. Blanchard-Desce, J. Lavergne, Kinetics of electron transfer and electrochromic change during the redox transition of the photosynthetic oxygen-evolving complex, Biochim. Biophys. Acta 1184 (1994) 178–192.